Functional specialization of gut CD103+ dendritic cells in the regulation of tissue-selective T cell homing

Bengt Johansson-Lindbom,[1] Marcus Svensson,[1] Oliver Pabst,[2] Caroline Palmqvist,[1] Gabriel Marquez,[3] Reinhold Förster,[2] and William W. Agace[1]

[1]Immunology Section, Lund University, BMC I-13, 221 84 Lund, Sweden
[2]Institute of Immunology, Hannover Medical School, 30625 Hannover, Germany
[3]Departamento de Immunologia y Oncologia, Centro Nacional de Biotecnologia/Consejo Superior de Investigaciones Cientificas, Universidad Autonoma de Madrid, Cantoblanco, 28040 Madrid, Spain

Gut-associated lymphoid tissue (GALT) dendritic cells (DCs) display a unique ability to generate CCR9$^+\alpha_4\beta_7^+$ gut-tropic CD8$^+$ effector T cells. We demonstrate efficient induction of CCR9 and $\alpha_4\beta_7$ on CD8$^+$ T cells in mesenteric lymph nodes (MLNs) after oral but not intraperitoneal (i.p.) antigen administration indicating differential targeting of DCs via the oral route. In vitro, lamina propria (LP)–derived DCs were more potent than MLN or Peyer's patch DCs in their ability to generate CCR9$^+\alpha_4\beta_7^+$ CD8$^+$ T cells. The integrin α chain CD103 (α_E) was expressed on almost all LP DCs, a subset of MLN DCs, but on few splenic DCs. CD103$^+$ MLN DCs were reduced in number in CCR7$^{-/-}$ mice and, although CD8$^+$ T cells proliferated in the MLNs of CCR7$^{-/-}$ mice after i.p. but not oral antigen administration, they failed to express CCR9 and had reduced levels of $\alpha_4\beta_7$. Strikingly, although CD103$^+$ and CD103$^-$ MLN DCs were equally potent at inducing CD8$^+$ T cell proliferation and IFN-γ production, only CD103$^+$ DCs were capable of generating gut-tropic CD8$^+$ effector T cells in vitro. Collectively, these results demonstrate a unique function for LP-derived CD103$^+$ MLN DCs in the generation of gut-tropic effector T cells.

CORRESPONDENCE
William W. Agace:
William.Agace@immuno.lu.se

Abbreviations used: 7-AAD, 7-amino-actinomycin D; CFSE, carboxyfluorescein diacetate succinimidyl ester; CT, cholera toxin; GALT, gut-associated lymphoid tissue; IEL, intraepithelial lymphocyte; LP, lamina propria; MLN, mesenteric LN; PLN, peripheral lymph node; PP, Peyer's patch.

Antigen-dependent differentiation of naive T cells in lymphoid organs leads to the generation of effector T cells exhibiting a de novo capacity to enter peripheral extralymphoid tissues (1). Effector T cells generated in different lymphoid organs display distinct tissue tropism, a feature that appears to be regulated by an organ-specific induction of adhesion molecules and chemokine receptors during T cell priming (2–4). For example, T cells activated in mesenteric LNs (MLNs) draining the gut acquire high-level expression of the integrin $\alpha_4\beta_7$ and the chemokine receptor CCR9, and these molecules are important for their subsequent localization to the small intestine (3, 5, 6). Conversely, T cells activated in skin-draining LNs acquire expression of E- and P-selectin ligands and CCR4 (2, 7) molecules that appear to direct T cells into inflamed skin (8–10).

DCs are critical for the generation of tissue-tropic effector T cell subsets. Thus, MLN or Peyer's patch (PP) DCs are necessary and sufficient for the generation of CCR9$^+\alpha_4\beta_7^+$ CD62L$^-$ gut-homing T cells in vitro, whereas T cells activated by antigen-pulsed skin-draining peripheral LN (PLN) DCs are induced to express E- and P-selectin ligands (5, 7, 11, 12). Gut-associated lymphoid tissue (GALT), but not splenic, DCs were recently shown to convert dietary vitamin A to retinoic acid, which in turn induced T cell expression of CCR9 and $\alpha_4\beta_7$ (13). Thus, the expression of retinoid dehydrogenase enzymes, catalyzing the sequential oxidation of vitamin A via retinal to retinoic acid appears in part to underlie their selective ability to generate gut-tropic T cells (13). Consistent with this possibility, T cells primed with fixed PP DCs failed to express CCR9 or $\alpha_4\beta_7$ (14). The site and underlying signals where GALT DCs are imprinted with their ability to generate gut-tropic T cells remain unknown. Indeed, sorting of GALT DCs based on well-established DC subset markers (CD8α and CD11b) indicates that all DCs resident within GALT have the ability to generate gut-tropic T cells (5, 14).

Here, we show that the capacity to generate gut-tropic $CD8^+$ effector T cells is present already among DCs in the small intestinal lamina propria (LP). Further, we identify a distinct subset of LP-derived DCs within the MLNs that express the epithelial–T cell associated integrin CD103 and have a unique capacity among MLN DCs to generate gut-homing T cells.

RESULTS

Oral administration of antigen leads to an efficient generation of $CCR9^+\alpha_4\beta_7^+$ gut-tropic $CD8^+$ T cells

CCR9 and $\alpha_4\beta_7$ are poorly induced on $CD8^+$ T cells proliferating in the MLNs after i.p. administration of antigen alone (5). To examine the generation of $CCR9^+\alpha_4\beta_7^+$ T cells after oral antigen administration, TCR-transgenic OVA-specific OT-I cells were transferred into recipient mice, and the frequencies of OT-I cells expressing CCR9 and $\alpha_4\beta_7$ in MLNs were examined 3 d after i.p. or oral administration of OVA (Fig. 1, A–C). Administration of OVA i.p. leads to a poor induction of CCR9 on responding T cells, and this was enhanced by coadministration of LPS (Fig. 1, B and C) as previously described (3, 5). In contrast, oral administration of OVA led to a strong induction of CCR9 on responding T cells both in the absence and presence of the mucosal adjuvant cholera toxin (CT; Fig. 1, B and C). A higher percentage of OT-I cells expressed CCR9 after antigen administration via the oral route as compared with the i.p. route, as well as when comparing carboxyfluorescein diacetate succinimidyl ester (CFSE)–labeled cells that had undergone the same number of cell divisions (not depicted), demonstrating that these differences do not reflect changes in OT-I cell cycle progression. Finally, expression of $\alpha_4\beta_7$ on the transferred OT-I cells conformed to the same pattern as observed for CCR9, although the difference between oral and i.p. immunization was less pronounced.

CCR9 plays a central role in the recruitment of activated $CD8^+$ T cells to the small intestinal epithelium after i.p. administration of OVA and adjuvant (3, 5). To determine whether CCR9 is important for this recruitment process of the immunization regime used, WT and $CCR9^{-/-}$ OT-I cells were cotransferred into WT recipient mice, and the ratio of the transferred cells in the MLN and intraepithelial lymphocyte (IEL) compartments was determined 3 d after oral or i.p. immunization in the absence or presence of adjuvant. Although CCR9 deficiency had no impact on the antigen-specific activation and expansion of OT-I cells in MLNs, the $CCR9^{-/-}$ OT-I cells were severely impaired in

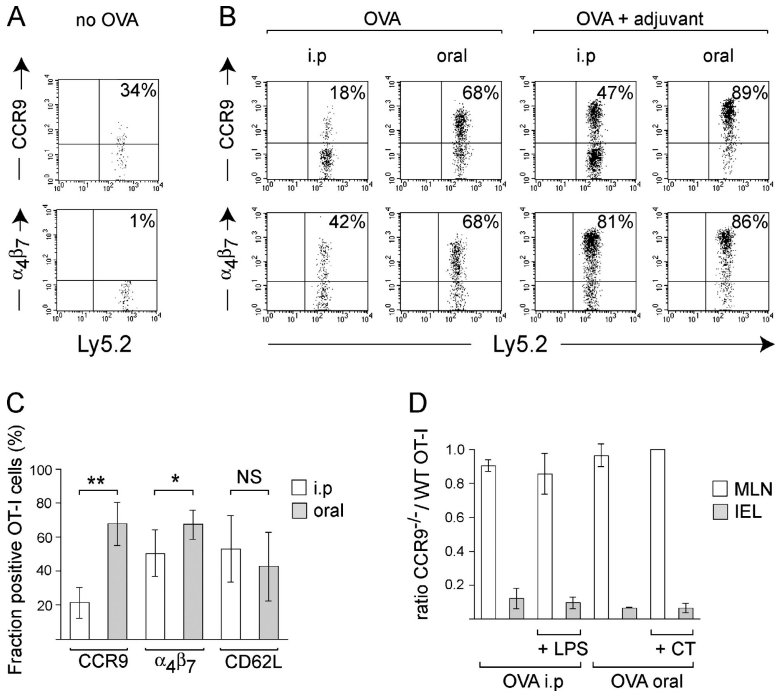

Figure 1. Efficient and adjuvant-independent generation of $CCR9^+\alpha4\beta7^+$ gut-homing T cells in the MLNs after oral administration of antigen. After adoptive transfer of OT-I cells (A–C) or an equal number of $CCR9^{-/-}$ and WT OT-I cells (D), recipient mice were injected i.p. with 5 mg OVA ± 50 μg LPS or given 50 mg OVA ± 20 μg CT orally. 3 d later, donor cells in MLNs (A–C) or MLNs and the small intestinal epithelium (D) were analyzed by flow cytometry. (A and B) Expression of CCR9 and $\alpha_4\beta_7$ by OT-I cells in MLNs. Numbers indicate the percentages of positive cells. One representative experiment of between five and seven performed. (C) Pooled results from mice receiving OVA alone orally (shaded bars) or i.p. (open bars). Mean ± SD of between five and seven experiments with three to four mice in each experiment. *, $P < 0.05$; **, $P < 0.005$. (D) Ratio of $CCR9^{-/-}$ to WT OT-I cells in the MLNs and IEL compartment. Mean ± SD of three separate experiments with three mice per group in each experiment.

their ability to enter the small intestinal epithelium after both oral and i.p. immunization in the absence or presence of adjuvant (Fig. 1 D).

LP DCs efficiently generate CCR9$^+\alpha_4\beta_7^+$ CD8$^+$ T cells in vitro

The efficient induction of CCR9 and $\alpha_4\beta_7$ on CD8$^+$ T cells in the MLNs after oral compared with i.p. antigen administration suggested that these two immunization routes were inducing differential DC migration/activation or preferentially targeting different DC populations. There was no difference in the number or phenotype (CD40, CD80, CD86, and CD103 expression) of CD11c$^+$MHC class II$^+$ DCs in the MLNs 24 h after administration of OVA i.p. (5 mg) or orally (50 mg; unpublished data), indicating that differences resulting from oral versus i.p. antigen administration were caused by differential DC targeting. DCs are numerous throughout the intestinal LP and are thought to play an important role in the sampling and processing of oral antigen (15). Furthermore, LP DCs migrate from the intestinal LP to the MLNs under steady-state conditions, and this migration process is enhanced after oral administration of CT and after i.v. injection of LPS (16–18). We therefore determined whether LP DCs were capable of generating CCR9$^+\alpha_4\beta_7^+$ CD8$^+$ T cells in vitro. To obtain sufficient numbers of LP DCs for in vitro studies, DCs were expanded in vivo by s.c. injection of Flt3L-producing melanoma cells, as previously

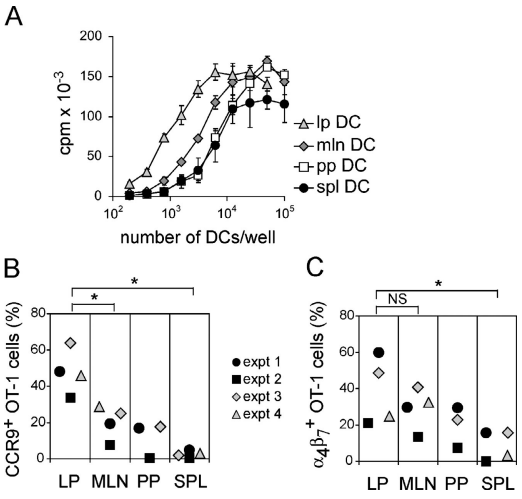

Figure 2. LP dendritic cells are potent in generating CCR9$^+\alpha4\beta7^+$ CD8$^+$ T cells. OT-I cells were activated in vitro with SIINFEKL peptide–pulsed DCs purified from LP, MLNs, PP, or spleen. (A) OT-I cell proliferation in response to a graded number of indicated DCs as assessed by quantification of *methyl*-[^{3}H]thymidine incorporation. Values represent mean ± SD. (B) CCR9 and (C) $\alpha_4\beta_7$ expression by CFSE-labeled OT-I cells was determined by flow cytometry after 4–5 d of co-culture with DCs. The percentage of positive cells among dividing OT-I cells is presented. DCs from Flt3L-treated mice were used in all experiments except experiment (expt) 4 in (B) and (C), where DCs were purified from pooled tissues of 10 untreated mice. *, $P < 0.05$. SPL, spleen.

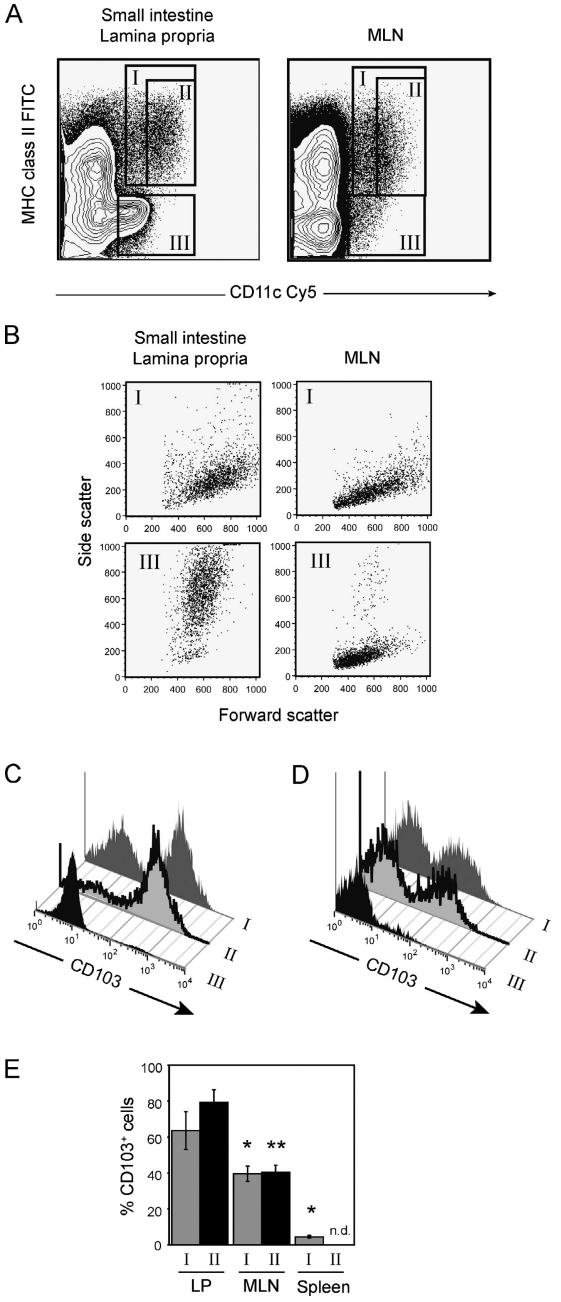

Figure 3. CD103 is expressed by the majority of LP DCs and a subset of MLN DCs. Leukocytes were isolated from the small intestinal LP, MLNs, and spleen and analyzed by flow cytometry using 7-AAD, anti–MHC class II–FITC, anti-CD11c–APC, and anti-CD103–PE mAbs. (A) Identification of CD11c$^+$MHC class II$^+$ (region I), CD11c^{high}MHC class II$^+$ (region II), and CD11c^{low}MHC class II$^-$ (region III) cells after gating on 7-AAD$^-$ (live) cells. (B) Light scatter properties of the indicated populations of cells. (C–D) Representative histograms showing CD103 expression by LP cells (C) and MLN cells (D) using the region definitions depicted in (A). (E) Statistical analysis of CD103 expression by CD11c$^+$MHC class II$^+$ (region I) and CD11c^{high}MHC class II$^+$ (region II) DCs from LP, MLNs, and spleen (mean ± SD; $n = 9$ for LP and MLNs, $n = 6$ for spleen). *, $P < 0.0005$; **, $P < 0.0001$ compared with LP equivalent. n.d., not done.

described (11). LP, MLN, PP, and splenic DCs, pulsed with OVA peptide, all induced efficient OT-I T cell proliferation (Fig. 2 A). Phenotypic analysis of proliferating OT-I cells demonstrated that LP DCs were by far the most efficient at generating CCR9$^+$ OT-I cells, followed by MLN and PP DCs (Fig. 2 B). The greater capacity of LP DCs to induce CCR9 on T cells was not caused by differences in cell cycling, as similar differences were observed when comparing CFSE-labeled T cells that had undergone the same number of cell divisions (unpublished data). All intestinal DC subsets induced expression of $\alpha_4\beta_7$ by the OT-I cells and did not substantially differ in this capacity (Fig. 2 C). OT-I cells activated by splenic DCs failed to express CCR9 and displayed relatively low levels of $\alpha_4\beta_7$ induction (Fig. 2, B and C), which was consistent with our previous results (5). Finally, data observed with Flt3L-treated mice were confirmed in one experiment using untreated mice, indicating that this procedure did not affect the outcome of our experiments (Fig. 2, B and C, experiment [expt] 4).

Small intestinal LP DCs express the integrin CD103

Given the more pronounced ability of LP DCs, as compared with MLN and PP DCs, to generate $\alpha_4\beta_7{}^+$CCR9$^+$ gut-homing T cells, it seemed conceivable that the capacity of MLN DCs to confer gut tropism to T cells is associated with the presence of an LP-derived subset in the MLNs. We therefore performed extensive phenotypic analysis of LP, MLN, and splenic DCs in an attempt to identify a marker for LP-derived DCs in the MLNs. One of the molecules we examined was the integrin CD103 ($\alpha_E\beta_7$) because it is expressed by rat DCs in most epithelial tissues (19), has previously been reported to be expressed by murine LP DCs (20), and is up-regulated on effector CD8$^+$ T cells soon after their entry into the small intestinal epithelium (21). CD103 was expressed by 80% of the CD11c^{high}MHC class II$^+$ DCs (region II) in LP and by 64% of the total CD11c$^+$MHC class II$^+$ LP DCs (region I; Fig. 3, A–E). In the MLNs, a substantially lower fraction of the CD11c$^+$MHC class II$^+$ DCs expressed CD103, and splenic DCs were largely CD103$^-$ (Fig. 3, D and E), which is in agreement with the results of Kilshaw (20). In the LP, an additional and distinct subset of CD11c^{low}MHC class II$^-$ cells that displayed the light scatter properties of granulocytes was identified (Fig. 3, A and B, region III). Only 5 ± 4% of these granular cells expressed CD103 (mean ± SD; $n = 9$; not depicted), and they were not present in the LP DC preparation used in the experiments shown in Fig. 2. Because these cells were not present in the MLNs (Fig. 3, A and B), we have not examined them further.

To confirm in situ the presence of CD103$^+$ DCs within the small intestinal LP, immunofluorescent labeling of tissue sections was performed (Fig. 4). In initial studies using a primary anti-CD11c mAb combined with secondary detection reagents, an abundant number of CD11c$^+$ cells were detected within the LP (not depicted). As many of these cells likely correspond to the numerous CD11c^{low}MHC class II$^-$ granular cells detected by flow cytometry (see Fig. 3 A, region III), we used a less sensitive, directly fluorochrome-labeled mAb against CD11c to detect just the CD11c^{high}

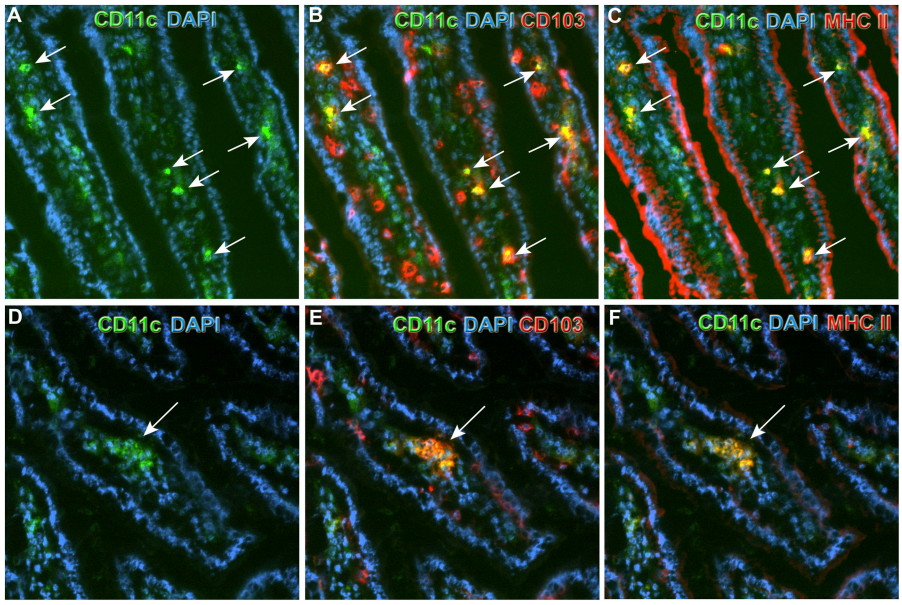

Figure 4. In situ expression of CD103 by LP DCs. Cryostat sections of the small intestinal jejunum of 8-wk-old C57BL/6 mice were analyzed for expression of CD11c, MHC class II, and CD103 by four-color immunofluorescence using DAPI for visualization of nuclei. Images show overlays of CD11c (green) and DAPI (blue) either alone (A and D) or in combination with CD103 (red; B and E) or MHC class II (red; C and F). CD11c$^+$MHC class II$^+$ DCs coexpressing CD103 (arrows) were found in the LP of the villi either as scattered cells (A–C) or in clusters (D–F). The contrast and γ parameters have been modified for CD11c- and MHC class II–derived fluorescence in order to balance the high intensity of the CD103 staining.

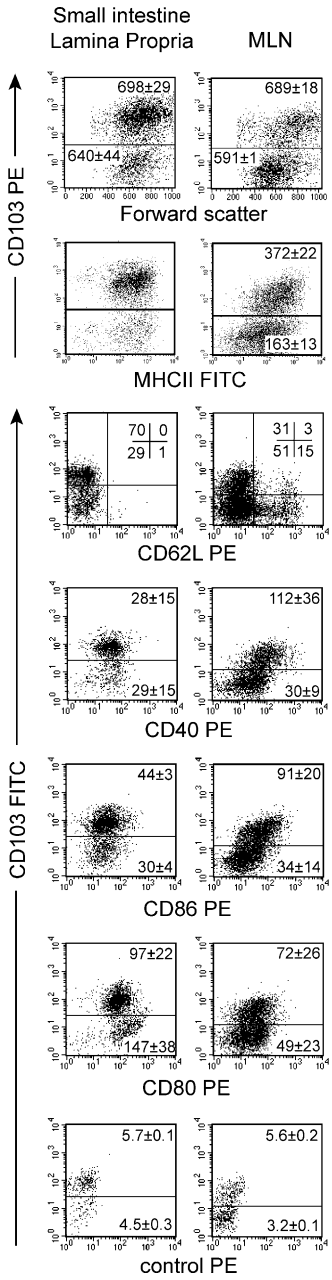

Figure 5. Phenotype of CD103$^+$ and CD103$^-$ DCs in the small intestinal LP and MLNs. Leukocytes were isolated from the small intestinal LP and MLNs, incubated with Cy5-conjugated anti-CD11c mAb, 7-AAD, and mAbs against the indicated proteins, and analyzed by flow cytometry. Expression levels of these proteins are shown after gating on 7-AAD$^-$ (live) and CD11c$^+$ (MLN) or CD11c^{high} (LP) cells. Because the flow cytometer was equipped with four photomultiplier tubes for fluorescence only, we could not include an MHC class II staining in these analyses. CD11c^{low} LP cells were therefore not considered because these include the MHC class II$^-$ and granular cells contained within region III that is shown in Fig. 3 A. The numbers indicate mean fluorescence intensity ± SD, except for the CD62L analysis, which indicates the percentage of cells in each quadrant.

cells. Consistent with the FACS data, the vast majority of these CD11c^{high}MHC class II$^+$ DCs within the LP expressed CD103 (Fig. 4).

Phenotypic analysis of CD103$^+$ DCs in the MLNs showed these cells to express high levels of MHC class II compared with their CD103$^-$ counterparts and higher, but still moderate, levels of CD40 and CD86 (Fig. 5). In the LP, all DCs expressed relatively low levels of CD40 and CD86 regardless of their expression of CD103, whereas CD103$^-$ LP DCs consistently expressed higher levels of CD80 than their CD103$^+$ counterparts or MLN DCs. CD62L expression, which is required for DC entry into the LNs directly from the blood stream (22), was confined to the CD103$^-$ DCs in MLNs and absent from all LP DCs (Fig. 5).

Collectively, there is a striking phenotypic resemblance between the CD103$^+$ MLN DCs and the previously described MHC class II^{high} semimature skin-derived DCs present in skin-draining LNs (23–25). Chemokine receptor CCR7 is required for migration of these skin-resident DCs to draining LNs under both steady-state and inflammatory conditions (25, 26). We therefore examined the frequency of CD11c$^+$MHC class II$^+$ DCs expressing CD103 in the MLNs of CCR7$^{-/-}$ and WT mice. The total number of CD11c$^+$MHC class II$^+$ DCs was reduced by 70% in the MLNs of CCR7$^{-/-}$ compared with WT mice. Furthermore, only 18 ± 4% of the MLN DCs in CCR7$^{-/-}$ mice expressed CD103, compared with 36 ± 3% of MLN DCs in WT mice (mean ± SD; $n = 5$ in each group). Thus, although the MLNs of CCR7$^{-/-}$ mice had a reduced total number of DCs compared with WT mice, there was a more pronounced reduction in the CD103$^+$ DC population. In contrast, the total number of CD11c^{high}MHC class II$^+$ LP DCs that expressed CD103 was similar in WT and CCR7$^{-/-}$ mice (unpublished data).

Generation of gut-homing T cells in MLNs requires a CCR7-dependent immigration of APCs

Next we used CCR7$^{-/-}$mice for adoptive transfer experiments. We have observed that OVA-specific CD4$^+$ T cells fail to proliferate in the MLNs of CCR7$^{-/-}$ mice after oral administration of OVA (unpublished data), indicating that DC migration from the gut mucosa to the MLNs is perturbed in these mice. Similarly, OT-I cells failed to proliferate in the MLNs of CCR7$^{-/-}$ mice after oral administration of OVA and CT (unpublished data). Nevertheless, OT-I cells proliferated equally well in the MLNs of CCR7$^{-/-}$ and WT mice after i.p. administration of OVA and LPS (Fig. 6 A). Collectively, these results suggest that CCR7 is required for DC migration from the intestinal LP to the draining MLNs and that this process is necessary for CD8$^+$ T cell priming in the MLNs after oral immunization.

If LP-derived DCs are critical for the generation of gut-tropic T cells in the MLNs, one would thus expect T cells primed in the MLNs of CCR7$^{-/-}$ mice to fail to express CCR9. Consistent with this possibility, after i.p. immuniza-

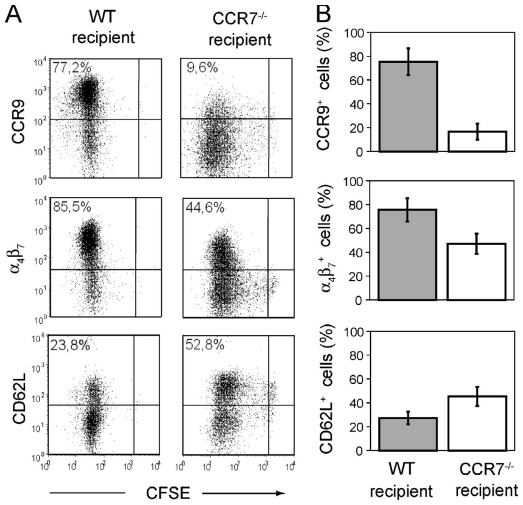

Figure 6. CD8$^+$ T cells primed in the MLNs of CCR7$^{-/-}$ mice fail to adopt a gut-tropic phenotype. CFSE-labeled OT-I cells were adoptively transferred into WT or CCR7$^{-/-}$ recipient mice. 3 d after i.p. immunization with OVA and LPS, MLNs were collected, and the phenotype of OT-I cells was determined by flow cytometry. (A) Representative data of CCR9, $\alpha_4\beta_7$, and CD62L expression by divided OT-I cells in the MLNs of WT versus CCR7$^{-/-}$ recipient mice. The CFSE gate is set to distinguish dividing from nondividing cells and is based on the CFSE intensity of OT-I cells in the PLNs of recipient mice (that do not divide) 3 d after oral OVA administration. The percentages indicate divided cells that express the markers shown. (B) Mean values ± SD obtained with three mice in each group.

tion with OVA and LPS, OT-I cells in the MLNs of WT mice expressed CCR9, whereas OT-I cells proliferating in the MLNs of CCR7$^{-/-}$ mice failed to express this receptor (Fig. 6, A and B). Induction of $\alpha_4\beta_7$ and loss of CD62L on OT-I cells in the MLNs of CCR7$^{-/-}$ mice was also reduced, but to a lesser extent.

CD103$^+$ but not CD103$^-$ MLN DCs generate CCR9$^+\alpha_4\beta_7^{high}$ CD8$^+$ T cells

Collectively, this line of experiments strongly suggested that CD103$^+$ DCs derived from the intestinal LP are important for the generation of gut-tropic T cells in the MLNs. To directly address this possibility, CD103$^+$ and CD103$^-$ DCs were sorted from the MLNs (Fig. 7 A) and pulsed with OVA peptide, and their ability to induce CCR9 and $\alpha_4\beta_7$ on responding OT-I cells was examined (Fig. 7). Both DC populations induced similar OT-I T cell proliferation, down-regulation of CD62L, and a similar percentage of IFN-γ–producing OT-I cells (Fig. 7, B, C, and F). In marked contrast, only CD103$^+$ MLN DCs were capable of inducing CCR9 on responding OT-I cells (Fig. 7, D and F) and were also more efficient in their ability to induce $\alpha_4\beta_7$ expression by the T cells, although this difference was less dramatic than observed for CCR9 (Fig. 7 D*)*. Because $\alpha_4\beta_7$ expression displays slow expression kinetics in vitro as compared with in vivo (11), we expanded the DC-primed OT-I cells by supplementing the cultures with IL-7 and IL-15 (27, 28). Although CCR9 levels were maintained after 3 d of expansion, a greater fraction of OT-I cells expressed $\alpha_4\beta_7$. In addition, a large proportion of OT-I cells activated by CD103$^-$ MLN DCs acquired expression of this integrin, although the proportion and levels remained lower than on OT-I cells activated by CD103$^+$ MLN DCs (Fig. 7, E and F). Finally, CD103$^+$ MLN DCs also selectively induced CCR9 on responding CD4$^+$ OT-II cells (Fig. 7 D); however, in contrast to OT-I cells, both DC subsets induced similar levels of $\alpha_4\beta_7$ on responding OT-II cells after primary activation (Fig. 7 D) or after expansion with IL-7 and IL-15 (unpublished data). Collectively, these results demonstrate a unique ability of CD103$^+$ MLN DCs in generating gut-tropic effector T cells.

DISCUSSION

We have identified a distinct subset of DCs expressing the integrin α chain CD103 that are responsible for generating CCR9$^+\alpha_4\beta_7^{high}$ gut-homing T cells in the MLNs. Most strikingly, CD103$^-$ DCs, which include the majority of MLN DCs, can prime both CD4$^+$ and CD8$^+$ T cells in vitro but fail to induce CCR9 on these cells. We further demonstrated that, regardless of the immunization regime being used, CCR9-deficient CD8$^+$ T cells are heavily disadvantaged in their capacity to enter the small intestinal epithelium, as compared with their CCR9-sufficient counterparts. Collectively, these results identify CD103$^+$ DCs as potential novel targets for regulating T cell accumulation within the intestinal mucosa.

Several results from the current study suggest that murine CD103$^+$ DCs in the MLNs derive from the intestinal LP. First, LP DCs, as CD103$^+$ MLN DCs, were potent generators of gut-tropic T cells in vitro. Second, CD103 was expressed on almost all CD11c^{high}MHC class II$^+$ LP DCs. Third, the percentage of DCs that expressed CD103 was considerably reduced in the MLNs of CCR7$^{-/-}$ mice. Finally, there was a phenotypic resemblance between the CD103$^+$ MLN DCs identified in the present study and the previously described skin-derived MHC class II^{high} semimature DCs in skin-draining LNs (23–25). Consistent with their LP origin, CD103 is expressed on almost all DCs in rat gut–draining LNs (19). We think it unlikely that CD103$^+$ MLN DCs derive from PP, because in our hands PP DCs were not as potent as MLN DCs at generating gut-tropic T cells, and the percentage of DCs expressing CD103 in the PP did not exceed those in the MLNs (unpublished data). Indeed, recent data in pigs suggest that few if any DCs migrate from the PP to the MLNs (29), and the number of LP, but not PP, DCs is heavily reduced after i.v. injection of LPS into mice (18).

The origin of the CD103$^-$ MLN DCs remains elusive. We believe that the CD103$^-$ LP DCs derive from isolated lymphoid follicles (30) or represent recently recruited DCs that have yet to express CD103 and that these cells are not a major

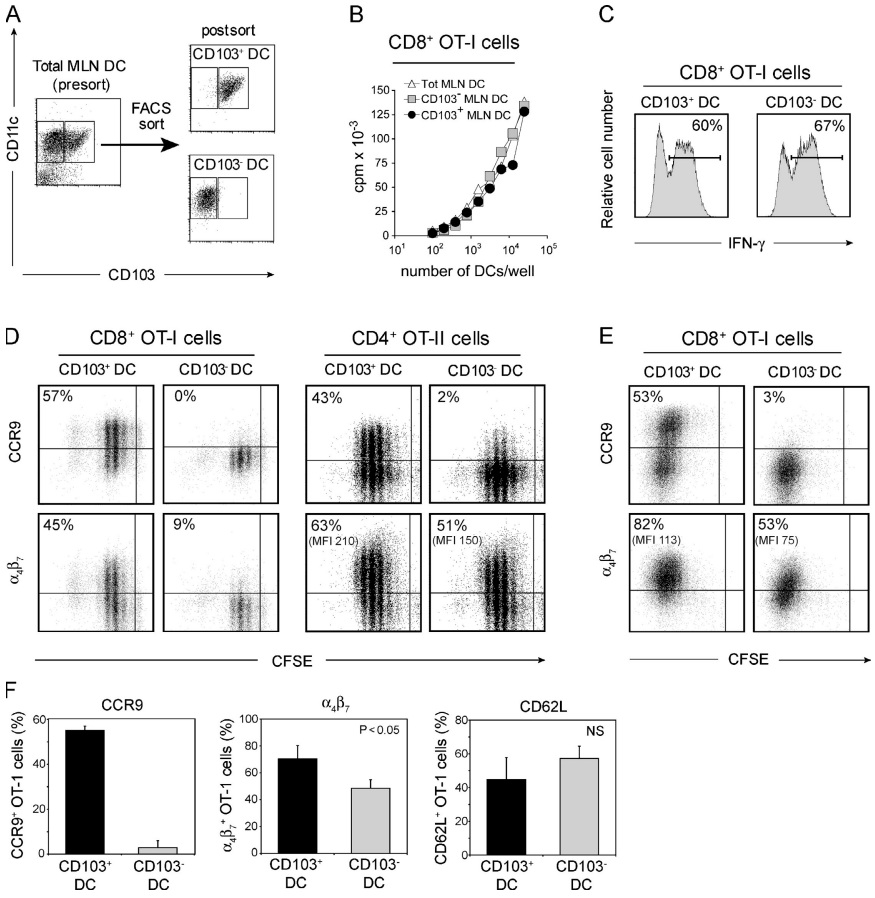

Figure 7. CD103$^+$ but not CD103$^-$ MLN DCs can generate gut-tropic CCR9$^+\alpha4\beta7^{high}$ T cells. (A) CD11c$^+$ DCs were enriched from MLNs using anti-CD11c magnetic bead cell sorting, incubated with fluorescently labeled mAbs against CD11c and CD103, and sorted into CD103$^+$ and CD103$^-$ DCs by FACS. (B–F) Indicated DC subsets were loaded with OVA peptide and co-cultured with CD8$^+$ OT-I or CD4$^+$ OT-II cells. (B) Proliferation of OT-I cells responding to a graded number of DCs was determined by *methyl*-[^{3}H]thymidine incorporation. One representative experiment of three performed is shown. (C) IFN-γ production by OT-I cells was determined by flow cytometry after expansion with IL-7 and IL-15. Percentages shown indicate OT-I cells expressing IFN-γ. (D–F) CFSE-labeled OT-I or OT-II cells were cultured with CD103$^+$ or CD103$^-$ DCs for 4–5 d (D) and further expanded in IL-7 and IL-15 for 3 d (E). Expression of CCR9, $\alpha_4\beta_7$, and CD62L by responding T cells was then analyzed by flow cytometry. (D and E) Results are from one representative experiment of four (OT-I) and two (OT-II) performed. The percentages indicate divided cells expressing the indicated markers. (F) Mean ± SD from four separate experiments in which expression of CCR9 and CD62L was analyzed after the primary DC culture, and α4β7 was analyzed after further expansion in IL-7 and IL-15.

source of CD103$^-$ MLN DCs. This belief is based on the finding that CD103$^-$ MLN DCs express far lower levels of MHC class II compared with CD103$^-$ LP DCs, display a very different phenotype than their CD103$^+$ MLN DC counterparts, and previous results that rat gut–draining lymph leukocytes depleted of CD103$^+$ cells are extremely poor in stimulating the primary mixed lymphocyte reaction (19), suggesting that few, if any, rat CD103$^-$ LP DCs migrate into the MLNs. The expression of CD62L by CD103$^-$ DCs in the MLNs indicates that at least some of these cells have entered directly from the blood via high endothelial venules, as previously reported to occur in popliteal LNs during viral infection (22).

The anatomical location and specific signals involved in imprinting MLN DCs with the ability to generate gut-tropic T cells are currently unknown. Clearly, these signals are not ubiquitously present within the MLNs, as CD103$^-$ MLN DCs were incapable of generating gut-tropic T cells. Furthermore, the ability of LP DCs to generate gut-tropic T cells strongly suggests that imprinting occurs before DC entry into the MLNs. In this regard, the association of CD103 with a DC's ability to generate gut-tropic T cells may provide a clue. CD103 (α_E) is the α chain of the $\alpha_E\beta_7$ integrin, expressed on the majority of human and mouse intestinal lymphocytes (31, 32), and mediates their adhesion to intestinal epithelial cells via interactions with E-cadherin (33). Importantly, effector CD8$^+$ T cells do not express CD103 before their entry into the intestinal mucosa but rapidly up-regulate this integrin after localizing to the intestinal epithelium (21). CD8$^+$ T cells expressing a dominant-negative TGF-βII receptor express reduced levels of CD103 after their entry into

the intestinal epithelium (34), indicating an important role for TGF-β, potentially derived from intestinal epithelial cells (35), in CD103 induction. Should CD103 be a marker of DCs that have been exposed to epithelial cells and TGF-β, it would seem likely that epithelial-derived factors also play an important role in imprinting them with an ability to generate gut-tropic T cells. An additional, although as we believe, less likely possibility is that a subset of DC precursors that have already been imprinted with an ability to generate gut-tropic T cells selectively localize to the intestinal LP.

Although only $CD103^+$ MLN DCs induced CCR9 on responding OT-I and OT-II cells, both $CD103^+$ and $CD103^-$ MLN DCs were capable of inducing $\alpha_4\beta_7$. These findings are consistent with several recent studies demonstrating a less stringent requirement for the induction of $\alpha_4\beta_7$ compared with CCR9. Indeed, $\alpha_4\beta_7$ is induced on T cells after prolonged activation in vitro by DCs from skin-draining LNs (14, 36). Because $\alpha_4\beta_7$ is detected on adoptively transferred $CD4^+$ or $CD8^+$ T cells in the MLNs but not PLNs after immunization of recipient mice (2, 5), $\alpha_4\beta_7$ expression appears to be more stringently regulated during immune responses in vivo. Nevertheless, T cells primed in the MLNs of $CCR7^{-/-}$ mice, which contain few $CD103^+$ DCs, failed to express CCR9 but showed a less dramatic reduction in $\alpha_4\beta_7$ expression compared with T cells primed in the MLNs of WT mice. Because both $\alpha_4\beta_7$ and CCR9 induction on T cells is dependent on intestinal DC production of retinoic acid (13), a potential explanation for these findings is that $\alpha_4\beta_7$ requires lower levels of retinoic acid as compared with CCR9 for its induction and that the $CD103^-$ MLN DCs can produce low quantities of retinoic acid. Because of the limited number of cells obtained after purification and cell sorting of $CD103^+$ and $CD103^-$ MLN DCs, we have not been able to examine the amount of retinoic acid generated by each of these populations. However, induction of $\alpha_4\beta_7$ by lower levels of retinoic acid could potentially be explained through synergistic signals provided by co-stimulatory molecules. Indeed, up-regulation of $\alpha_4\beta_7$ in vivo is partially blocked in the presence of a neutralizing mAb against the OX40L (37), suggesting that OX40 signaling may act in synergy with retinoic acid to trigger expression of $\alpha_4\beta_7$ by T cells. Consistent with a CD40-dependent expression of OX40L by DCs (38), we have also found that a neutralizing antibody to CD40L reduces the number of $\alpha_4\beta_7^+$ OT-I cells by ~50% after co-culture with MLN DCs, whereas CCR9 expression is unaffected by this treatment (unpublished data).

Several studies have demonstrated expression of CD103 on DCs both within and outside the small intestine (19, 20). In the rat, CD103 was originally identified through the mAb OX-62 raised against veiled cells obtained from the cannulated thoracic duct of mesenteric lymphadenectomized animals; however, it is also present on DCs in the thymus, cervical LNs, interstitium of the lung, portal triads of the liver, glomeruli of the liver, islet of Langerhans of the pancreas, and epithelium of choroid plexus, but not in heart and skeletal muscle (19). A similar distribution of $CD103^+$ DCs has been reported in the mouse (20). We also confirm the findings of Kilshaw (20) that murine splenic DCs, in apparent contrast to DCs in the rat spleen (19), are largely $CD103^-$. Thus, as with effector $CD8^+$ T cells, CD103 expression on DCs appears to be primarily restricted to epithelial tissues or LNs draining such tissues. Finally, we have found that ~20% of DCs in skin-draining LNs express CD103 and that this frequency is also dramatically reduced in $CCR7^{-/-}$ mice (unpublished data). Collectively, these results indicate that $CD103^+$ DCs may represent a unique population of DCs associated with epithelial tissues and that these cells are capable of migrating to local draining LNs. In this regard it will be of considerable interest to determine whether $CD103^+$ DCs in LNs draining distinct epithelial tissues generate effector T cells with tropism for that particular site.

Finally, our results suggest that the efficient generation of gut-tropic T cells after oral compared with i.p. antigen administration is caused by a differential targeting of DCs. Furthermore, experiments in $CCR7^{-/-}$ mice revealed that oral-administered OVA does not reach the MLNs in soluble form in sufficient quantity to induce OT-I cell proliferation but must be transported to the MLNs by DCs. Thus, the enhanced generation of $CCR9^+\alpha_4\beta_7^{high}$ OT-I cells after oral immunization compared with i.p. immunization likely reflects enhanced antigen presentation by LP-derived DCs in the MLNs. Indeed, intestinal DCs display a pronounced migration into the draining MLNs under steady-state conditions (18, 39). How then is adjuvant functioning to enhance the generation of gut-tropic T cells? Because both oral CT and systemic LPS administration induce DC migration from the small intestinal LP into the draining MLNs (16–18), adjuvant likely promotes the generation of gut-tropic T cells by enhancing the number of intestinally imprinted LP-derived DCs in the MLNs. At this point, we cannot exclude the possibility that adjuvant also functions directly to mature the gut-imprinting ability of $CD103^+$ DCs within the MLNs; however, it is notable that i.v. injection of LPS into rats almost completely emptied the small intestinal LP of DCs within 12 h, whereas the phenotype of the DCs in the gut-draining LNs and in the MLNs showed no apparent signs of maturation, as judged from expression levels of CD80 and CD86 (18).

In conclusion, we have demonstrated that the capacity to generate tissue-selective T cell subsets in the gut is highly restricted to a specialized subset of $CD103^+$ MLN DCs most likely originating from the small intestinal LP. The presence of $CD103^+$ DCs in LNs draining other epithelial tissues suggests that these cells may also provide important (but different) cues for T cell migration at these sites. Our results indicate that targeting the $CD103^+$ intestinal DCs may provide a novel means of regulating intestinal immune responses. This may be of particular importance in the development of oral vaccines and in the treatment of chronic inflammatory bowel disease.

MATERIALS AND METHODS

Mice. OT-I, C57BL/6 (Ly5.1), and C57BL/6 mice were obtained from the Jackson Laboratory. OT-II mice were provided by M.-J. Wick (Gothenburg University, Gothenburg, Sweden). $CCR9^{-/-}$ OT-I (provided by A. Wurbel and B. Malissen, Institut national de la santé et de la recherche médicale, Paris, France) and $Ly5.1^{+}Ly5.2^{+}$ OT-I mice were generated as previously described (5). $CCR7^{-/-}$ mice have been described previously (26). All mice were bred and maintained at the BioMedical Center animal facility of Lund University or at the central animal facility of Hannover Medical School, and all animal work was approved by the local ethical review boards in Lund and Hannover, respectively.

Reagents. In vitro cell culturing was performed in RPMI 1640 with 10% FCS, 2 mM L-Glutamine, 10 mM Hepes, 1 mM sodium pyruvate, 50 μM β-mercaptoethanol, 100 U/ml penicillin G, 100 μg/ml streptomycin sulfate, and 50 μg/ml gentamicin (all reagents were obtained from GIBCO BRL), hereafter referred to as complete R10 medium. Also, HBSS was obtained from GIBCO BRL. OVA (grade VI; Sigma-Aldrich) was purified from endotoxins by Detoxi-Gel chromatography (Pierce Chemical Co.). Synthetic peptides were purchased from Innovagen. LPS (*Escherichia coli*, serotype 055:B55), CT (from *Vibrio cholerae*), DNase I, collagenase type IV and VIII, 7-amino-actinomycin D (7-AAD), PMA, ionomycin, and Brefeldin A were obtained from Sigma-Aldrich. Recombinant cytokines were purchased from R&D Systems, CFSE was purchased from Invitrogen, and *methyl*-[^{3}H]thymidine was purchased from GE Healthcare. The following antibodies were obtained from BD Biosciences: PE- and FITC-conjugated anti-CD103 (M290, IgG2a), unconjugated or PE-conjugated anti-$\alpha_4\beta_7$ (DATK32, rat IgG2a), PE- or APC-conjugated anti-CD62L (MEL-14, rat IgG2a), biotinylated anti-CD80 (16-10A1, hamster IgG), PE-conjugated anti–IFN-γ (XMG1.2, rat IgG1), PE-conjugated anti-Ly5.1 (A20, mouse IgG2a), FITC-conjugated anti-Ly5.2 (104, mouse IgG2a), and PE-conjugated antikeyhole limpet hemocyanin (isotype control; A110-2, rat IgG2a). PE-labeled anti-Ly5.2 (clone 104) was purchased from eBioscience. Anti-CCR9 (K629, polyclonal rabbit IgG) has been described previously (40). The following mAbs were produced from the hybridomas, purified, and labeled according to standard procedures: FITC anti–MHC class II (clone M5/114.15.2, rat IgG2b), Cy5 anti-CD11c (clone N418, hamster IgG), biotin anti-CD40 (clone FGK45, rat IgG2a), and biotin anti-CD86 (clone GL1, rat IgG2a). Primary rabbit IgG and rat IgG2a antibodies were revealed using biotinylated goat anti–rabbit IgG (polyclonal; Jackson ImmunoResearch Laboratories) and biotinylated mouse anti–rat IgG2a (RG7/1.30; BD Biosciences), respectively, followed by PE- or APC-labeled streptavidin (BD Biosciences).

DC purification. For in vivo expansion of DCs, C57BL/6 mice were injected s.c. on the dorsal flank with 15–20 × 10^6 Flt3L-secreting B16 melanoma cells/mouse as previously described (11). Mice were killed 8–10 d later, and the indicated organs were removed and used for isolation of DCs.

In experiments depicted in Fig. 2, DCs were purified from Flt3L-treated C57BL/6 mice. In all other experiments, untreated C57BL/6 mice were used. LNs and spleens were first cut into small pieces and then treated with 500 μg/ml collagenase IV and 50 U/ml DNase I diluted in RPM 1640 with 10% FCS and antibiotics. Enzymatic digestion was performed for 45 min at 37°C on an orbital shaker at 250 revolutions per minute. The remaining tissue was mechanically minced, and resulting cell suspensions were pooled and filtered through a 70-μm cell strainer. Cells were washed in PBS containing 2% FCS and 2 mM EDTA, and this buffer was used in all subsequent purification steps. Erythrocytes were removed from spleen cells by standard Ficoll-Paque density centrifugation (Pharmacia Fine Chemicals). DCs were then immunomagnetically sorted using anti-CD11c–conjugated magnetic beads and sequential passage over 2 LS columns, according to the manufacturer's protocol (Miltenyi Biotec).

DCs were isolated from the small intestine by enzymatic digestion of the LP after removal of PP and epithelial cells. In brief, after extensive flushing with HBSS and removal of PP, the small intestine was cut longitudinally and then into 5-mm pieces. Epithelial cells were removed by incubating the tissue for 15 min at 37°C with 2 mM EDTA in HBSS supplemented with 10% FCS, followed by vigorous shaking for 10 s. The samples were filtered using a nylon mesh and subjected to further EDTA treatment for a total of three times. To release LP leukocytes, the remaining tissue was incubated for 45 min at 37°C with 100 U/ml collagenase type VIII and 50 U/ml DNase I diluted in HBSS containing 10% FCS and 10 mM Hepes. After digestion, the samples were shaken vigorously for 10 s, supernatants were collected by filtration through a nylon mesh, and tissue was subjected to a second round of enzymatic digestion. Leukocytes were further enriched on a 40:70 Percoll gradient where the interface was collected after centrifugation at 600 *g* for 20 min. DCs were finally immunomagnetically sorted as described in the previous section. For all DC preparations, >95% of positively selected cells expressed CD11c and >90% were $CD11c^{+}$MHC class II^{+}, as assessed by flow cytometry.

For sorting of MLN DCs into $CD103^{+}$ and $CD103^{-}$ subsets, $CD11c^{+}$ cells were first enriched from total MLN cells by immunomagnetic cell sorting on a single LS column. Positively selected cells were then incubated with PE-conjugated anti-CD11c mAb (HL3, Hamster IgG; BD Biosciences), FITC-conjugated anti-CD103, and 7-AAD and sorted on a FACSVantage (Becton Dickinson) into $7\text{-AAD}^{-}CD11c^{+}CD103^{+}$ and $7\text{-AAD}^{-}CD11c^{+}CD103^{-}$ fractions. Purity of sorted $CD103^{+}$ and $CD103^{-}$ DCs routinely exceeded 90 and 95%, respectively.

In vitro cultures. Splenic $CD8\beta^{+}$ and $CD4^{+}$ T cells were obtained from OT-I and OT-II mice, respectively, using biotinylated anti-CD8β mAb (53–5.8, rat IgG1; BD Biosciences), followed by streptavidin-conjugated magnetic beads or anti-CD4–conjugated beads, followed by purification on LS columns according to the manufacturer's protocol (Miltenyi Biotec). Purified DCs from MLNs, PP, LP, or spleen were incubated for 1 h at 37°C with either 1 nM $OVA_{257–264}$ SIINFEKL peptide (recognized by the OT-I TCR in the context of K^b) or 1 μM $OVA_{323–339}$ ISQAVHAAHAEINEAGR peptide (recognized by the OT-II TCR in the context of $I\text{-}A^b$). After extensive washing, 10^5 peptide-pulsed DCs were co-cultured with 2 × 10^5 CFSE-labeled OT-I or OT-II cells in a final volume of 200 μl complete R10 medium using a flatbottom 96-well plate. Primary cultures were analyzed by flow cytometry at day 4 of co-culture, and secondary cultures were analyzed after an additional 3 d of expansion in 1 ml of fresh, complete R10 medium supplemented with 10 ng/ml each of IL-7 and IL-15.

Proliferation of 10^5 OT-I cells/well in triplicate wells in response to a graded number of peptide-pulsed DCs was quantified during a 36-h period of co-culture by measuring *methyl*-[^{3}H]thymidine incorporation (1 μCi/well) into DNA during the final 16 h of culture. For this purpose, cells were co-cultured in a flatbottom 96-well plate, and incorporated radioactivity was counted in a liquid scintillation counter (Wallac 1450; Microbeta).

Adoptive transfer experiments. 3 × 10^6 $CD8\beta^{+}$ OT-I cells were injected i.v. into C57BL/6 or $CCR7^{-/-}$ recipient mice. For adoptive transfers into the $Ly5.1^{+}$ C57BL/6 recipients, we used $Ly5.2^{+}$ OT-I cells or an equal number of $Ly5.2^{+}$ $CCR9^{-/-}$ OT-I and $Ly5.1^{+}Ly5.2^{+}$ WT OT-I cells. The $Ly5.2^{+}$ $CCR7^{-/-}$– and C57BL/6-recipient mice received CFSE-labeled $Ly5.1^{+}Ly5.2^{+}$ OT-I cells. 1 d after OT-I cell transfer, recipient mice were immunized either orally with 50 mg OVA with or without 20 μg CT or i.p. with 5 mg OVA with or without 50 μg LPS. 3 d later, mice were killed, and organs and tissues were collected. Isolation of small intestinal IEL and lymphocytes from LNs was performed as previously described (3). Donor OT-I cells were analyzed by flow cytometry and distinguished from the recipient cells based on Ly5.1/Ly5.2 expression.

Flow cytometry analysis. To determine the phenotype of DCs in LNs, spleen, and the small intestine LP, single-cell suspensions were prepared from the respective organ/tissue according to the protocols described in DC purification section. Adoptively transferred $Ly5.2^{+}$ and $Ly5.1^{+}Ly5.2^{+}$ OT-I cells

were detected using FITC- or PE-labeled anti-Ly5.2 mAb and PE-conjugated anti-Ly5.1 mAb, respectively. PBS supplemented with 2% FCS and 2 mM EDTA was used for all incubations and washing procedures. All samples were preincubated with 2 μg/ml of anti-FcR mAb (2.4G2), and all incubations were performed on ice for 30 min with the viability marker 7-AAD included in the final incubation step. Analysis of intracellular IFN-γ was performed after a 4-h restimulation with 50 ng/ml PMA and 1 μg/ml ionomycin in the presence of 10 μg/ml Brefeldin A, followed by fixation and permeabilization with 4% paraformaldehyde and 0.5% saponin (Sigma-Aldrich). Data was acquired using a flow cytometer (FACSCalibur; Becton Dickinson), and data analysis was performed with the CellQuest (Becton Dickinson), FlowJo (Tree Star, Inc.), and FCSExpress (De Novo Software) software.

Tissue staining. Acetone-fixed cryostat sections of the small intestine jejunum were quenched with 0.3% H_2O_2, preincubated with 5% rat serum in TBST (0.1 M Tris, pH 7.5, 0.15 M NaCl, 0.1% Tween 20) and blocked sequentially with 0.001% avidin (wt/vol) and 0.001% biotin (wt/vol) in PBS. Sections were then incubated for 1 h with APC-conjugated anti-CD11c, FITC-conjugated anti–MHC class II, and with biotinylated anti-CD103 mAbs diluted in TBST containing 5% rat serum. The anti-CD103 mAb was then visualized by first applying horseradish peroxidase–labeled streptavidin and then Alexa 546–conjugated tyramide, according to the manufacturer's recommendations (Invitrogen). Slides were counterstained with DAPI and mounted, and images were acquired using an Axiovert 200M microscope and the Axiovision software (Carl Zeiss MicroImaging, Inc.).

Statistical analysis. All statistical analyses were performed using the two-tailed Mann-Whitney U test.

We would like to thank Drs. A. Wurbel and B. Malissen for providing the CCR9$^{-/-}$ mice and Dr. A. Mowat for valuable input during the preparation of this manuscript.

This work was supported by grants from the Swedish Medical Research Council (VR-Medicine; 2003-5126); the Wellcome Trust (075571/Z/04/Z); the Crafoordska, Österlund, Åke Wiberg, Nanna Svartz, and Kocks foundations; the Swedish Medical and Royal Physiographic Societies; the Swedish foundation for Strategic Research "Microbes and Man" and Individual Grant for the Advancement of Research Leaders II program; and the Deutsche Forschungsgemeinschaft (SFB621-TPA1).

The authors have no conflicting financial interests.

Submitted: 31 May 2005
Accepted: 25 August 2005

REFERENCES

1. Kunkel, E.J., and E.C. Butcher. 2002. Chemokines and the tissue-specific migration of lymphocytes. *Immunity*. 16:1–4.
2. Campbell, D.J., and E.C. Butcher. 2002. Rapid acquisition of tissue-specific homing phenotypes by CD4$^+$ T cells activated in cutaneous or mucosal lymphoid tissues. *J. Exp. Med*. 195:135–141.
3. Svensson, M., J. Marsal, A. Ericsson, L. Carramolino, T. Broden, G. Marquez, and W.W. Agace. 2002. CCL25 mediates the localization of recently activated CD8alphabeta(+) lymphocytes to the small-intestinal mucosa. *J. Clin. Invest*. 110:1113–1121.
4. Calzascia, T., F. Masson, W. Di Berardino-Besson, E. Contassot, R. Wilmotte, M. Aurrand-Lions, C. Ruegg, P.Y. Dietrich, and P.R. Walker. 2005. Homing phenotypes of tumor-specific CD8 T cells are predetermined at the tumor site by crosspresenting APCs. *Immunity*. 22:175–184.
5. Johansson-Lindbom, B., M. Svensson, M.-A. Wurbel, B. Malissen, G. Márquez, and W. Agace. 2003. Selective generation of gut-tropic T cells in gut-associated lymphoid tissue (GALT); requirement for GALT dendritic cells and adjuvant. *J. Exp. Med*. 198:963–969.
6. Lefrancois, L., C.M. Parker, S. Olson, W. Muller, N. Wagner, M.P. Schon, and L. Puddington. 1999. The role of β7 integrins in CD8 T cell trafficking during an antiviral immune response. *J. Exp. Med*. 189: 1631–1638.
7. Dudda, J.C., J.C. Simon, and S. Martin. 2004. Dendritic cell immunization route determines CD8+ T cell trafficking to inflamed skin: role for tissue microenvironment and dendritic cells in establishment of T cell-homing subsets. *J. Immunol*. 172:857–863.
8. Reiss, Y., A.E. Proudfoot, C.A. Power, J.J. Campbell, and E.C. Butcher. 2001. CC chemokine receptor (CCR)4 and the CCR10 ligand cutaneous T cell–attracting chemokine (CTACK) in lymphocyte trafficking to inflamed skin. *J. Exp. Med*. 194:1541–1547.
9. Tietz, W., Y. Allemand, E. Borges, D. von Laer, R. Hallmann, D. Vestweber, and A. Hamann. 1998. CD4+ T cells migrate into inflamed skin only if they express ligands for E- and P-selectin. *J. Immunol*. 161:963–970.
10. Campbell, J.J., G. Haraldsen, J. Pan, J. Rottman, S. Qin, P. Ponath, D.P. Andrew, R. Warnke, N. Ruffing, N. Kassam, et al. 1999. The chemokine receptor CCR4 in vascular recognition by cutaneous but not intestinal memory T cells. *Nature*. 400:776–780.
11. Mora, J.R., M.R. Bono, N. Manjunath, W. Weninger, L.L. Cavanagh, M. Rosemblatt, and U.H. von Andrian. 2003. Selective imprinting of gut-homing T cells by Peyer's patch dendritic cells. *Nature*. 424:88–93.
12. Stagg, A.J., M.A. Kamm, and S.C. Knight. 2002. Intestinal dendritic cells increase T cell expression of alpha4beta7 integrin. *Eur. J. Immunol*. 32:1445–1454.
13. Iwata, M., A. Hirakiyama, Y. Eshima, H. Kagechika, C. Kato, and S.Y. Song. 2004. Retinoic acid imprints gut-homing specificity on T cells. *Immunity*. 21:527–538.
14. Mora, J.R., G. Cheng, D. Picarella, M. Briskin, N. Buchanan, and U.H. von Andrian. 2005. Reciprocal and dynamic control of CD8 T cell homing by dendritic cells from skin- and gut-associated lymphoid tissues. *J. Exp. Med*. 201:303–316.
15. Mowat, A.M. 2005. Dendritic cells and immune responses to orally administered antigens. *Vaccine*. 23:1797–1799.
16. Anjuere, F., C. Luci, M. Lebens, D. Rousseau, C. Hervouet, G. Milon, J. Holmgren, C. Ardavin, and C. Czerkinsky. 2004. In vivo adjuvant-induced mobilization and maturation of gut dendritic cells after oral administration of cholera toxin. *J. Immunol*. 173:5103–5111.
17. MacPherson, G.G., S. Fossum, and B. Harrison. 1989. Properties of lymph-borne (veiled) dendritic cells in culture. II. Expression of the IL-2 receptor: role of GM-CSF. *Immunology*. 68:108–113.
18. Turnbull, E.L., U. Yrlid, C.D. Jenkins, and G.G. Macpherson. 2005. Intestinal dendritic cell subsets: differential effects of systemic TLR4 stimulation on migratory fate and activation in vivo. *J. Immunol*. 174: 1374–1384.
19. Brenan, M., and M. Puklavec. 1992. The MRC OX-62 antigen: a useful marker in the purification of rat veiled cells with the biochemical properties of an integrin. *J. Exp. Med*. 175:1457–1465.
20. Kilshaw, P.J. 1993. Expression of the mucosal T cell integrin alpha M290 beta 7 by a major subpopulation of dendritic cells in mice. *Eur. J. Immunol*. 23:3365–3368.
21. Ericsson, A., M. Svensson, A. Arya, and W.W. Agace. 2004. CCL25/CCR9 promotes the induction and function of CD103 on intestinal intraepithelial lymphocytes. *Eur. J. Immunol*. 34:2720–2729.
22. Martin, P., S.R. Ruiz, G.M. del Hoyo, F. Anjuere, H.H. Vargas, M. Lopez-Bravo, and C. Ardavin. 2002. Dramatic increase in lymph node dendritic cell number during infection by the mouse mammary tumor virus occurs by a CD62L-dependent blood-borne DC recruitment. *Blood*. 99:1282–1288.
23. Lutz, M.B., and G. Schuler. 2002. Immature, semi-mature and fully mature dendritic cells: which signals induce tolerance or immunity? *Trends Immunol*. 23:445–449.
24. Stoitzner, P., S. Holzmann, A.D. McLellan, L. Ivarsson, H. Stossel, M. Kapp, U. Kammerer, P. Douillard, E. Kampgen, F. Koch, et al. 2003. Visualization and characterization of migratory Langerhans cells in murine skin and lymph nodes by antibodies against Langerin/CD207. *J. Invest. Dermatol*. 120:266–274.
25. Ohl, L., M. Mohaupt, N. Czeloth, G. Hintzen, Z. Kiafard, J. Zwirner, T. Blankenstein, G. Henning, and R. Forster. 2004. CCR7 governs skin dendritic cell migration under inflammatory and steady-state conditions. *Immunity*. 21:279–288.

26. Forster, R., A. Schubel, D. Breitfeld, E. Kremmer, I. Renner-Muller, E. Wolf, and M. Lipp. 1999. CCR7 coordinates the primary immune response by establishing functional microenvironments in secondary lymphoid organs. *Cell*. 99:23–33.
27. Schluns, K.S., W.C. Kieper, S.C. Jameson, and L. Lefrancois. 2000. Interleukin-7 mediates the homeostasis of naive and memory CD8 T cells in vivo. *Nat. Immunol.* 1:426–432.
28. Zhang, X., S. Sun, I. Hwang, D.F. Tough, and J. Sprent. 1998. Potent and selective stimulation of memory-phenotype CD8+ T cells in vivo by IL-15. *Immunity*. 8:591–599.
29. Bimczok, D., E.N. Sowa, H. Faber-Zuschratter, R. Pabst, and H.J. Rothkotter. 2005. Site-specific expression of CD11b and SIRPalpha (CD172a) on dendritic cells: implications for their migration patterns in the gut immune system. *Eur. J. Immunol.* 35:1418–1427.
30. Pabst, O., H. Herbrand, T. Worbs, M. Friedrichsen, S. Yan, M.W. Hoffmann, H. Korner, G. Bernhardt, R. Pabst, and R. Forster. 2005. Cryptopatches and isolated lymphoid follicles: dynamic lymphoid tissues dispensable for the generation of intraepithelial lymphocytes. *Eur. J. Immunol.* 35:98–107.
31. Cerf-Bensussan, N., A. Jarry, N. Brousse, B. Lisowska-Grospierre, D. Guy-Grand, and C. Griscelli. 1987. A monoclonal antibody (HML-1) defining a novel membrane molecule present on human intestinal lymphocytes. *Eur. J. Immunol.* 17:1279–1285.
32. Kilshaw, P.J., and S.J. Murant. 1990. A new surface antigen on intraepithelial lymphocytes in the intestine. *Eur. J. Immunol.* 20:2201–2207.
33. Cepek, K.L., S.K. Shaw, C.M. Parker, G.J. Russell, J.S. Morrow, D.L. Rimm, and M.B. Brenner. 1994. Adhesion between epithelial cells and T lymphocytes mediated by E-cadherin and the alpha(E)beta(7) integrin. *Nature*. 372:190–193.
34. El-Asady, R., R. Yuan, K. Liu, D. Wang, R.E. Gress, P.J. Lucas, C.B. Drachenberg, and G.A. Hadley. 2005. TGF-β–dependent CD103 expression by $CD8^+$ T cells promotes selective destruction of the host intestinal epithelium during graft-versus-host disease. *J. Exp. Med.* 201:1647–1657.
35. Barnard, J.A., G.J. Warwick, L.I. Gold, Y.H. Chin, J.P. Cai, and X.M. Xu. 1993. Localization of transforming growth factor beta isoforms in the normal murine small intestine and colon. *Gastroenterology*. 105:67–73.
36. Dudda, J.C., A. Lembo, E. Bachtanian, J. Huehn, C. Siewert, A. Hamann, E. Kremmer, R. Forster, and S.F. Martin. 2005. Dendritic cells govern induction and reprogramming of polarized tissue-selective homing receptor patterns of T cells: important roles for soluble factors and tissue microenvironments. *Eur. J. Immunol.* 35:1056–1065.
37. Malmstrom, V., D. Shipton, B. Singh, A. Al-Shamkhani, M.J. Puklavec, A.N. Barclay, and F. Powrie. 2001. CD134L expression on dendritic cells in the mesenteric lymph nodes drives colitis in T cell-restored SCID mice. *J. Immunol.* 166:6972–6981.
38. Fillatreau, S., and D. Gray. 2003. T cell accumulation in B cell follicles is regulated by dendritic cells and is independent of B cell activation. *J. Exp. Med.* 197:195–206.
39. Huang, F.P., N. Platt, M. Wykes, J.R. Major, T.J. Powell, C.D. Jenkins, and G.G. MacPherson. 2000. A discrete subpopulation of dendritic cells transports apoptotic intestinal epithelial cells to T cell areas of mesenteric lymph nodes. *J. Exp. Med.* 191:435–444.
40. Carramolino, L., A. Zaballos, L. Kremer, R. Villares, P. Martin, C. Ardavin, A.C. Martinez, and G. Marquez. 2001. Expression of CCR9 beta-chemokine receptor is modulated in thymocyte differentiation and is selectively maintained in CD8(+) T cells from secondary lymphoid organs. *Blood*. 97:850–857.